

SPECTROPHOTOMETRIC STUDY OF COMPLEXATION EQUILIBRIA AND OF A METHOD FOR THE DETERMINATION OF Fe(III) IONS WITH 4-(2-PYRIDYLATO)RESORCINOL AND 4-(2-THIAZOLYLATO)RESORCINOL

Ellena RUSSEVA^a, Vlastimil KUBÁŇ and Lumír SOMMER

*Department of Analytical Chemistry,
Purkyně University, 611 37 Brno*

Received January 12th, 1978

The composition, molar absorption coefficients, equilibrium constants and stability constants for the MLH , ML , $M(LH)_2$ and ML_2 complexes have been determined graphically using slope-intercept transformations and numerically from the absorbance-pH curves and from the absorbance dependence on the component concentration, using the PRCEK III and SPEKTFOT programs, or from the continuous variation plots using the JOBCON program. The optimum conditions were found for a spectrophotometric determination of ferric ions with TAR and PAR reagents in pure solutions. The basic parameters of the analytical curves were evaluated using the STAT program.

N-heterocyclic azodyes substituted in the *ortho* position with respect to the azo-group are very sensitive and selective reagents for identification of iron ions¹⁻⁸ and also very sensitive and selective spectrophotometric reagents for the determination of iron ions⁹⁻³⁷. Ferrous and ferric ions react with these azodyes under similar conditions, ferric ions reacting in somewhat more acidic media ($\Delta pH 1-2$). The absorption spectra of ferrous and ferric ions with most of these reagents contain several absorption bands that are separated to varying degrees; the longest wavelength absorption band of Fe(II) often lies around 700-800 nm (e.g. PAN, PAR, etc.). In this region, only the complexes of Pd(II) and Co(III) with these reagents absorb radiation; consequently, iron ions can be selectively determined in the presence of many other ions without separation or the use of masking agents (EDTA, NTA). The high molar absorption coefficients (e.g. $\epsilon = 6 \cdot 10^4$ for the Fe-PAR complex), which can be further increased by formation of ion associates with quaternary ammonium salts (zephiramine, benzylidimethyl-tetradecylammonium chloride, etc.²⁰), also render this group of reagents advantageous for spectrophotometric determination of traces of iron in various materials, compared with common reagents, such as 1,10-phenanthroline, bathophenanthroline, ferrozine, etc.

Although this group of reagents (PAN, PAR, TAR, etc.) is often used for determination of iron, the literature is ambiguous and unclear concerning the complexation equilibria in solution and data on the optimum conditions for the determination vary widely. The present paper therefore presents a detailed spectrophotometric study of

* Present address: Institute of General and Inorganic Chemistry, Bulgarian Academy of Sciences, Sofia 1113.

these equilibria with 4-(2-thiazolylazo)resorcinol and 4-(2-pyridylazo)resorcinol in 30% v/v ethanol or in aqueous medium. To determine the basic characteristics of the complexes, the absorbance curves were interpreted by combining graphical and numerical methods. The conditions for the determination of Fe(II) in pure solutions were critically evaluated and statistical parameters were determined for the calibration curves.

EXPERIMENTAL

Chemicals and Instruments

4-(2-Pyridylazo)resorcinol (PAR) and 4-(2-thiazolylazo)resorcinol (TAR) were obtained from Lachema, Brno and recrystallized several times from ethanol before use³⁸. The contents of the reagent active components (91.5 and 98.5%, respectively) were determined by elemental analysis (C, H, N) and by photometric titration with a standard Cu(II) solution^{26,38}. The chromatographic purity of the preparations was tested by TLC on Silufol_{EP} (Kavalier, Votice, Czechoslovakia) in several elution systems³⁹. Stock solutions of PAR and TAR with concentrations of $2 \cdot 10^{-4}$ – $5 \cdot 10^{-3}$ M were prepared by dissolving the solid substances or in a small amount of dimethylformamide and 1M-NaOH, diluting the solution formed with redistilled water (PAR) or ethanol (TAR) to the appropriate volume. The DMF concentration in the experimental solutions did not exceed 0.1–0.2% vol.

A 0.1008M stock solution of $\text{Fe}(\text{NO}_3)_3$ was prepared by dissolving solid $\text{Fe}(\text{NO}_3)_3 \cdot 9 \text{ H}_2\text{O}$ *p.a.* (Lachema, Brno), doubly recrystallized from 1M- HNO_2 , in 1M- HNO_3 . The Fe(III) concentration was determined gravimetrically.

The ethanol used contained 5% v/v methanol. The other chemicals were commercial substances of *p.a.* purity. Some of them were purified by recrystallization (KNO_3 , $\text{Fe}(\text{NO}_3)_3$, etc.) and distillation (DMF, ethanol). The ionic strength of the solutions was maintained at 0.10 by addition of 1M- HNO_3 , KNO_3 and NaOH.

The solution acidity was measured by PHM4d and PHM 64 pH-meters (Radiometer, Denmark) with G 202 B glass and a K 401 saturated calomel electrode. The instrument was calibrated regularly using a set of standard aqueous buffers (phthalate, pH 4.01, phosphate, pH 6.48 and borate, pH 9.18, at 25°C). The absorption spectra were obtained on a Carry 118A double-beam recording spectrophotometer (Varian, Australia) or on a Unicam SP 700 instrument (Pye Unicam, England) at 25°C. All other measurements were carried out with single-beam SF-D2 (LOMO, USSR) and Unicam SP 500 (Pye Unicam, England) spectrophotometers. The measurement of the absorbance curves $A = f(\text{pH})$, $A = f(c_M)$, $A = f(c_L)$ and $A = f(x_T)$ by the classical method in volumetric flasks and in a special device for the measurement in a closed system was described earlier^{40–43}.

Methods

To determine the basic parameters of the absorbing species — the position of the absorption maxima and isobestic points, molar absorption coefficients, stoichiometry and the equilibrium or stability constants — the absorbance curves were interpreted graphically using the slope — intercept transformations⁴⁰. The results of the graphical methods were supplemented by the results of numerical data treatment using the PRCEK III program^{47,48} based on the linear least squares method. Using the linearity condition or the criterion of the lowest sum of the

squares of the deviations U and highest correlation coefficient r_{xy} , the stoichiometry of the complexes and the most probable mechanism of complex formation were found. From the intercepts and slopes of the appropriate linear dependences, the molar absorption coefficients and the reaction equilibrium constants were calculated. The principle and basic equations were given in earlier works⁴⁰⁻⁴³.

The results were supplemented by the values of the equilibrium constants, molar absorption coefficients and stoichiometric coefficients obtained from the numerical treatment of the continuous variation plots using the JOBCON program⁴⁹ based on the Likussar procedure^{44,45}.

Some ambiguous cases were treated by the SPEKTFOT general minimization program⁴⁶.

RESULTS

Acid-Base and Optical Properties of PAR and TAR

Four optically different species exist in aqueous or aqueous-alcoholic media, in dependence on the acidity of the medium. In strongly acidic media the H_3L^+ species exists, protonated on the heterocyclic nitrogen, then the molecular H_2L species, the HL^- species, which dissociates at the *p*-hydroxyl group and finally the L^{2-} species, dissociating at the *o*-hydroxyl group. With PAR, doubly protonated species H_4L^{2+} exist in addition to the previous ones, in concentrated sulphuric acid ($c_{\text{H}} > 3\text{M}$).

TABLE I

Survey of the Optical Characteristics of Individual Acid-Base Forms of 4-(2-Pyridylazo)resorcinol and 4-(2-Thiazolylazo)resorcinol

| Form | PAR ^a acidity, pH | TAR ^b | | |
|---------------------------|---------------------------------|--|-------------|---|
| | | λ_{max} , nm | acidity, pH | λ_{max} , nm |
| H_4L^{2+} | >3 M H^+ | 436 | — | — |
| H_3L^+ | >3 | 395(1), 452(0.3), 245(>3) | <1 | 481(1), 410(0.55), 280(>3) |
| H_2L | 4-5 | 386(1), 245(>3) | 2.5-4 | 438(1), 415(0.98), 230(<2) |
| HL^- | >4 | 414(1), 345(>3) | >7 | 480(1), 400(0.4), 308(0.1), 284(0.2), 240(>3) |
| L^{2-} | >10.5 | 488(1), 414(0.43), 354(0.06), 268(0.2), 220(0.4) | >9 | 513(1), 405(0.3), 313(0.1), 286-260 (0.2) |

^a Aqueous medium, ^b measured in 30% v/v ethanol, the data in parenthesis after the wavelength specify the relative molar absorption coefficients at the maximum, related to the longest wavelength absorption maximum.

For both reagents, the molar absorption coefficients of the individual acid-base forms were determined at wavelengths corresponding to the absorption maxima of the acid-base forms and of the Fe(III) complexes (495, 510, 520, 530, 540 and 570 nm for TAR and 400, 495, 510, 520, 535, 550, 570 and 705 nm for PAR) and the dissociation constants for the acid-base equilibria, using graphical methods and the PRCEK III program^{47,48}. Because of the instability of TAR in strongly acidic media (pH < 0) and the relatively low pK_{a1} value (~0.75), the deprotonation constant of TAR in 30% v/v ethanol was determined only for points at pH > 0.1 and at ionic strength I 1.0. Solutions of PAR were also unstable in neutral and weakly alkaline regions (pH = 7–8.5), but the determination of the dissociation constant was unaffected.

The optical and acid-base characteristics of the two ligands and comparison with the literature data are given in Tables I and II.

TABLE II
Survey of the Dissociation Constants of PAR and TAR in Various Media

| Equilibrium | pK_{a1} | PAR |
|-------------|-----------|--|
| H_3L/H_2L | pK_{a1} | $3.02 \pm 0.02^a, 2.7^b, 3.1^d, 2.3^e, 2.41^g, 3.03 \pm 0.04^o, 4.15^p$ |
| H_2L/HL | pK_{a2} | $5.56 \pm 0.01^a, 5.83^b, 5.5^c, 5.6^d, 6.9^e, 7.15^g, 7.0^h, 5.3^i, 5.48^j, 6.20^k, 5.9^l, 5.57^o, 6.15^p$ |
| HL/L | pK_{a3} | $11.98 \pm 0.02^a, 12.5^b, 12.3^c, 11.9^d, 12.4^e, 11.34^f, 13.0^g, 12.4^h, 12.3^i, 12.31^j, 11.50^k, 11.34^m, 12.5^n, 11.96^o, 11.98^p$ |
| | | TAR |
| H_3L/H_2L | pK_{a1} | $0.75 \pm 0.01^{a,r}, 0.75^q, 0.75^s, 1.17^t, 0.98^u, 0.88^x, 1.13^z, 1.65^{aa}, 0.84^{ab}, 1.06^{ac}$ |
| H_2L/HL | pK_{a2} | $6.51 \pm 0.04^{a,r}, 6.50^q, 6.56^s, 6.48^t, 6.23^u, 5.9^v, 6.40^w, 6.36^x, 6.53^y, 6.18^z, 7.37^{aa}, 6.36^{ab}, 6.56^{ab}, 7.25^{ac}$ |
| HL/L | pK_{a3} | $10.67 \pm 0.02^{a,r}, 10.65^q, 10.54^s, 10.77^t, 9.44^u, 10.3^v, 10.52^w, 10.68^x, 10.76^y, 9.88^z, 12.80^{aa}, 10.42^{ab}, 11.52^{ac}$ |

^a This work, aqueous medium, 25°C, $I = 0.10$ KNO₃; ^b ref.¹⁴; ^c ref.²⁴; ^d ref.²⁵; ^e ref.⁵¹, 50% dioxan; ^f ref.⁵³; ^g ref.²³, 50% dioxan; ^h ref.⁵², 50% dioxan; ⁱ ref.⁵⁴; ^j ref.⁵⁵, 50% dioxan; ^k ref.⁵⁵; ^l ref.⁵⁷, 30% DMF; ^m ref.⁵⁸; ⁿ ref.⁷; ^o ref.⁶⁰, aqueous medium, 25°C; 0.10 KNO₃; ^p ref.⁵⁹ 0.1% sodium laurate; ^r this work, conditions: see ^a), 30% ethanol medium; ^s ref.⁶⁰, 30% ethanol; ^q ref.⁶¹; ^u ref.⁶⁰; aqueous medium; ^v ref.⁶³, 20% methanol; ^w ref.³¹, 20% dioxan; ^x ref.⁶², 30% ethanol; ^y ref.²³, 50% methanol; ^z ref.⁶⁴, 2% dioxan; ^{aa} ref.⁶⁴, 50% dioxan; ^{ab} ref.⁶⁵, 30% DMF; ^{ac} 50% DMF, ref.⁶⁵.

Reaction of Fe(III) with TAR in 30% v/v Ethanol

The absorption maxima of the ligand (λ_{\max} 414 and 440 nm) in the absorption spectra of TAR solutions containing excess Fe(III) ion ($c_M/c_L = 40$ and 10, $c_L = 5 \cdot 10^{-5}$ M, $c_M = 2 \cdot 10^{-3}$ M or $5 \cdot 10^{-4}$ M, $I = 0.10$) disappear with increasing pH and chelate formation and an absorption band with a maximum at 450 nm and wide absorption band at 540 nm appear in a pH interval of 1–1.5 (Fig. 2, curves 14–19). Further maxima at 540, 478 and 330 nm appear at pH > 1.8. Both complexation equilibria are indicated by sharp isosbestic points at 390 and 440 nm. In the absorption spectra of equimolar solutions ($c_M = c_L = 5 \cdot 10^{-5}$ M) the ligand maxima are converted into complex maxima at 540 and 475 nm at pH > 3 (Figs 1 and 2) and the curves pass through an isosbestic point at 456 nm. With increasing pH a bathochromic shift of the shorter wavelength band occurs (λ_{\max} 482 nm) and the absorption band is perceptibly distorted at 540 nm. The curves pass through an isosbestic point at 436 nm. The distortion disappears at pH > 9.5 and at pH > 10.5 the absorption spectrum contains only the band of the pure anionic form of the ligand L^{2-} , with a maximum at 513 nm. In this pH interval the curves pass through an isosbestic point at 486 nm (Fig. 2, curves 10–13).

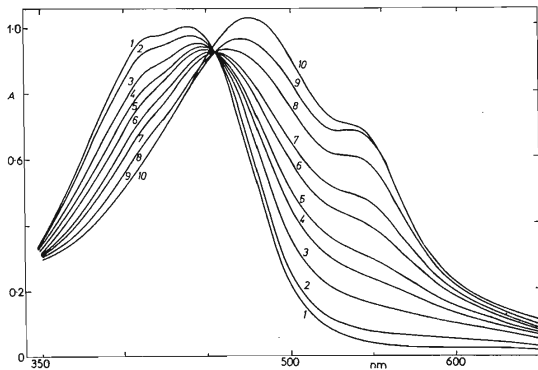


FIG. 1

Absorption Curves for Equimolar Solutions of Fe(III) with TAR in 30% v/v Ethanol Medium
 $c_M = c_L = 5 \cdot 00 \cdot 10^{-5}$ M, $I = 0.10$ (KNO_3 , HNO_3), $t = 25^\circ C$. Curve, pH; 1 1.30, 2 2.03, 3 2.27,
 4 2.54, 5 2.74, 6 3.02, 7 3.29, 8 3.57, 9 3.86, 10 4.12.

The absorption spectra of solutions with excess ligand ($c_M = 1 \cdot 10^{-6} M$, $c_L = 1 \cdot 10^{-5} M$, $c_L/c_M = 10$) at pH > 2 contain, in addition to the ligand absorption bands (415 and 438 nm), an absorption band of a complex at 540 nm. The curves pass through an isosbestic point at 450 nm. At pH > 5.2, an absorption maximum appears at 480 nm, whereas the maximum at 540 nm remains unchanged and the curves pass through an isosbestic point at 426 nm. Finally at pH > 9.5, the maximum shifts to 514 nm, corresponding to the maximum of fully ionized TAR. The isosbestic point lies at 482 nm.

The absorbance-pH curves of TAR solutions with excess Fe(III) ions, measured at 495, 510, 530, 540, 550 and 570 nm ($c_L = 5.04 \cdot 10^{-5} M$, $c_M/c_L = 50, 30, 20, 10, 8, 5$ and 1) indicate that the complex begins to form at pH 1.3. Within this pH range, the LH_3/LH_2 ligand equilibrium plays a role, which is manifested by non-symmetry of the $A = f(pH)$ curves at pH < 2. The complex formation is quantitative even in solutions with low concentration excesses ($c_M/c_L \geq 5$) of ferric ions (Fig. 3). The absorbance-pH curves of solutions with excess TAR ($c_L/c_M = 1, 5, 10$ and 20 at $c_M = 1.008 \cdot 10^{-5} M$) and equimolar solutions ($c_M = c_L = 5.04 \cdot 10^{-5}$ or $2.52 \cdot 10^{-5} M$) are slightly shifted to the neutral region (Fig. 4). Ligand dissociation, LH_3/LH_2 and

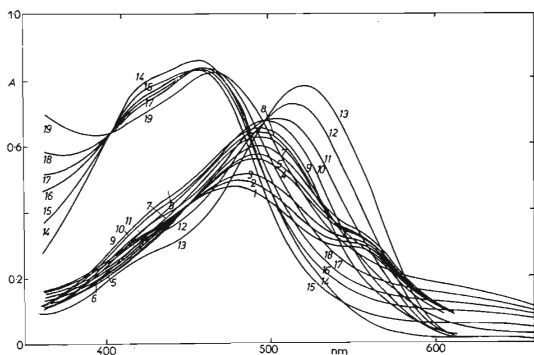


FIG. 2

Absorption Curves for Solutions of Fe(III) with TAR in 30% v/v Ethanol Medium

$c_M = c_L = 5.00 \cdot 10^{-5} M$ for curves 1-13, $c_M = 40 c_L = 2.00 \cdot 10^{-3} M$ for curves 14-19. Curve, pH: 1 4.18, 2 4.39, 3 4.62, 4 0, 5 4.88, 6 5.00, 7 5.28, 8 5.54, 9 5.83, 10 6.05, 11 6.34, 12 6.62, 13 7.08, 14 1.25, 15 1.40, 16 1.71, 17 1.94, 18 2.12, 19 2.32.

LH_2/LH plays a role only at the ends of the curves, at $\text{pH} < 2.5$ and $\text{pH} > 4.5$, causing an increase in the solution absorbance and non-symmetry of the curves that is especially significant at $\lambda < 530 \text{ nm}$.

The molar absorption coefficient and equilibrium constants were estimated approximately from the absorbances on the horizontal parts and from the position of the inflection points on the $\Delta A = f(\text{pH})$ curves⁴⁰. All these values, together with the dissociation constants and the molar absorption coefficients of the individual acid-base forms of the ligand, were used as the initial values for graphical interpretation by the slope-intercept method and for numerical calculation using the PRCEK III and SPEKTFOT programs⁴⁶⁻⁴⁸.

The most probable mechanism for the individual equilibria considered,

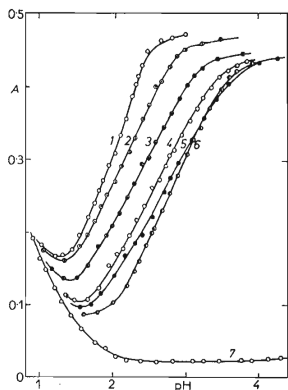
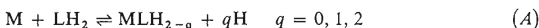


FIG. 3

Absorption-pH Curves of Fe(III) Solutions with TAR with Excess Ferric Ions in 30% v/v Ethanol Medium

$c_L = 5.00 \cdot 10^{-5} \text{ M}$ TAR, $I 0.10$ (KNO_3 , HNO_3), 540 nm, $t 25.00^\circ\text{C}$. Curve, $10^4(c_M)$, c_M/c_L : 1 25.0 50, 2 15.0 30, 3 10.0 20, 4 5.0 10, 5 4.0 8, 6 2.5 5, 7 0.0 ligand.

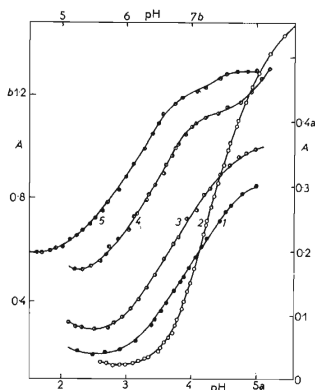
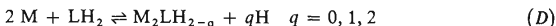


FIG. 4

Absorption-pH Curves of Fe(III) Solution with TAR at Excess Ligand

$c_M = 5.00 \cdot 10^{-5} \text{ M}$ for Curve 1, $c_M = 1.00 \cdot 10^{-5} \text{ M}$ for curves 2-5, $\lambda 530 \text{ nm}$ for curves 2 and 3, $\lambda 560 \text{ nm}$ for curves 1, 4 and 5. Curve, $10^4 \cdot c_L$, c_L/c_M ; module pH, module A: 1 0.50 5 aa, 2 0.00 10 aa, 3 1.00 aa, 4 2.00 2.0 aa + 0.1, 5 2.0 20 bb.



with simultaneous dissociation equilibrium



was tested only for wavelengths of 540 and 495 nm and for all concentration ratios, $c_M/c_L = 50 \rightarrow 1/20$, because of the tediousness of the calculation and long computing

TABLE III

Survey of the Equilibrium Constants for the Formation of Fe(III) Complexes with TAR in 30% v/v Ethanol

$t = 25^\circ\text{C}$, $I = 0.10\text{M-KNO}_3$.

| K | Conditions | $\log K$ | |
|---------------------------------------|---------------------|--------------------|--------------------|
| $k_{11H} = [MLH][H]/[M][LH_2]$ | 50 ^a | 0.62 ^b | 0.625 ^c |
| | 30 ^a | 0.60 ^b | 0.645 ^c |
| | 20 ^a | 0.71 ^b | 0.70 ^c |
| | 10 ^a | 0.68 ^b | 0.695 ^c |
| | 8 ^a | 0.77 ^b | 0.725 ^c |
| | 5 ^a | 0.70 ^b | 0.705 ^c |
| | 1.5; 2 ^e | 0.705 ^b | 0.72 ^c |
| | 3 ^e | 0.72 ^b | 0.74 ^c |
| <i>average</i> 0.67 | | | |
| $k_{12} = [ML_2H_2][H]^2/[M][LH_2]^2$ | 5 ^f | 0.64 ^b | 0.68 ^c |
| | 10 ^f | 0.70 ^b | 0.72 ^c |
| | 20 ^f | 0.72 ^b | 0.73 ^c |
| | 3 ^g | 0.79 ^b | 0.80 ^c |
| <i>average</i> 0.73 | | | |

^a Average of the values for wavelengths 495, 510, 520, 530, 540 and 550 nm from the absorbance-pH curves at $c_L = 5.00 \cdot 10^{-5}\text{M}$ TAR, the numbers specify the c_M/c_L ratio; ^b results of direct calculation from the inflection point; ^c results of direct and logarithmic analysis of the curves; ^d results obtained by the PRCEK III program as the mean of the values from the graphical and logarithmic curve interpretation, ^e average of the values for the above wavelengths obtained from the absorbance vs metal concentration curves, $A = f(c_M)$; ^f absorbance-pH curves with excess ligand, $A = f(pH)$, the average for wavelengths 495, 510, 530 and 550 nm; ^g $A = f(pH)$ curves for pH 3.00 and wavelengths 495, 510, 530 and 550 nm.

time required. The results of the graphical and numerical methods verify the existence of equilibrium (A) in solutions with excess Fe(III) ions and at pH > 1.8 with dissociation of one proton ($q = 1.0$) and the formation of protonated complex MLH. The conversion of complex MLH into nonprotonated complex ML could not be unambiguously verified on all the curves, as in solutions with excess Fe(III) ions the parts of the absorbance-pH curves at pH > 2.5–3 are considerably affected by hydrolysis of Fe(III) ions and the measurement is irreproducible. At higher excesses, a red-purple precipitate separates.

In solutions with excess TAR and in equimolar solutions, the optimum U and r_{xy} values were obtained for equilibrium (B) with bonding of two ligand molecules to one iron atom and dissociation of two protons, with formation of the doubly protonated $M(LH)_2$ complex.

The average values of the molar absorption coefficients and of the equilibrium constants for both complexes, obtained by the graphical methods and numerically

TABLE IV

Survey of the Molar Absorption Coefficients for the $Fe(LH)$ and $Fe(LH)_2$ Complexes with TAR in 30% v/v Ethanol

| Conditions and measuring method | Calculation method ^a | ϵ^{495} | ϵ^{510} | ϵ^{520} | ϵ^{530} | ϵ^{540} | ϵ^{550} |
|---|---------------------------------|------------------|------------------|------------------|------------------|------------------|------------------|
| $A = f(pH)$, $c_M \gg c_L$ | <i>A</i> | 17 915 | 14 420 | 12 350 | 10 620 | 9 900 | 8 280 |
| $c_M/c_L = 50, 30$ | <i>B</i> | 17 490 | 14 610 | 12 750 | 10 730 | 9 605 | 8 405 |
| $c_L = 5.00 \cdot 10^{-5} M$ | <i>C</i> | 19 625 | 14 810 | 12 608 | 10 705 | 9 370 | 8 375 |
| $A = f(pH)$, $c_M \gg c_L$ | <i>A</i> | 14 395 | 12 090 | 10 365 | 9 235 | 8 590 | 7 890 |
| $c_M/c_L = 20, 10, 8,$ 5.0, 3.0, $c_L 5.0 \cdot 10^{-5} M$ | <i>B</i> | 14 730 | 12 415 | 10 860 | 9 580 | 8 560 | 7 930 |
| $A = f(c_M)$, pH = 1.5, 2.0, 3.0 | <i>C</i> | 15 570 | 12 570 | 10 940 | 9 785 | 8 550 | 7 920 |
| $A = f(c_M)$, pH = 1.5, 2.0, 3.0 | <i>A</i> | 15 050 | 12 200 | 10 800 | 10 000 | 8 720 | 8 000 |
| $c_L = 5.00 \cdot 10^{-5} M$ | <i>B</i> | 15 270 | 12 500 | 10 920 | 10 420 | 8 600 | 8 000 |
| $A = f(c_L)$, pH = 3.0, 4.0, 5.5 | <i>C</i> | 15 920 | 12 790 | 11 010 | 10 050 | 8 720 | 8 120 |
| $A = f(pH)$, $c_L \gg c_M$ | <i>A</i> | 32 200 | 32 675 | | 29 825 | | 27 950 |
| $c_L/c_M = 10, 20, 5$ | <i>B</i> | 33 620 | 34 175 | | 30 120 | | 28 200 |
| $c_M = 1.008 \cdot 10^{-5} M$ | <i>C</i> | 33 580 | 34 420 | | 30 510 | | 28 605 |
| $A = f(c_L)$, pH = 3.0, 4.0, 5.5 | <i>A</i> | 33 190 | 33 980 | | 30 050 | | 27 800 |
| $c_M = 2.52 \cdot 10^{-5} M$ | <i>B</i> | 34 090 | 34 750 | | 31 450 | | 28 900 |
| | <i>C</i> | 34 170 | 34 930 | | 32 000 | | 28 960 |

^a Method *A*, direct calculation from the absorbance on the plateau $\epsilon = A_{02}/c_M$ or $\epsilon = A_{02}/c_L$; method *B*, results of the direct graphical analysis; method *C*, results obtained by direct graphical interpretation using the PRCEK III program.

using the PRCEK III and SPEKTFOT programs for the whole sets of the absorbance-pH curves and all wavelengths, are given in Tables III and IV. The individual values agree well. The graphical and numerical (the PRCEK III program) interpretation of the absorbance dependence on the ligand concentration, $\Delta A = f(c_L)$ (for $c_M = 2.52 \cdot 10^{-5} M$, $c_L = 1.0 \cdot 10^{-5} - 2.5 \cdot 10^{-4} M$, pH = 3.0, 4.0 and 5.5) verifies the existence of a complex with a M : L molar ratio of 1 : 2, which is formed according to equation (B) with dissociation of two protons. The absorbance *vs.* Fe(III) concentration curves, $A = f(c_M)$, measured in a strongly acid region ($c_L = 5 \cdot 10^{-5} M$, $c_M = 1.008 \cdot 10^{-5} - 1.008 \cdot 10^{-3} M$, pH = 1.5, 2.5 and 3.0) verify bonding of a single Fe(III) ion according to equilibrium (A), with dissociation of one proton and formation of the MLH complex at pH 1.5 and a mixture of the MLH and ML complexes at pH 2.5 and 3.0 (Fig. 5). The molar absorption coefficients and equilibrium constants are given in Tables III and IV.

The continuous variation plots, $\Delta A = f(x_L)$, for various wavelengths and pH values (pH = 2.0, 2.5, 3.0, 4.0, 4.5 and 9.0 for $c_0 = c_M + c_L = 1.008 \cdot 10^{-4} M$) exhibit absorption maxima at TAR mole fraction of $x_L = 0.60 - 0.70$, which verifies the

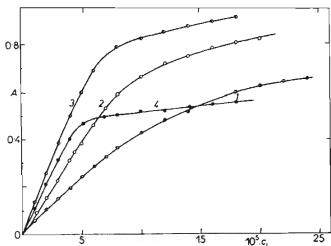


FIG. 5

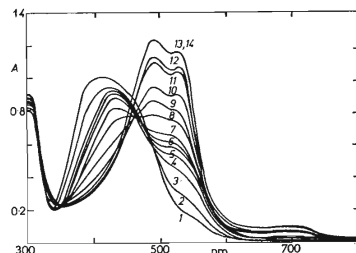
Absorbance-Ligand Concentration Curves
 $\Delta A = f(c_L)$ for Solutions of Fe(III) with
 TAR in 30% Ethanol

$c_M = 2.50 \cdot 10^{-5} M$, 540 nm, for other
 conditions see Fig. 3. Curve, pH: 1 3.50,
 2 4.00, 3 4.50, 4 5.50.

FIG. 6

Absorption Curves of Fe(III) Solutions with
 PAR in Aqueous Medium

$c_M = 2.00 \cdot 10^{-5} M$, $c_L = 5.00 \cdot 10^{-5} M$,
 $c_L/c_M = 2.5$, t 25°C, I 0.10 (KNO₃, HNO₃).
 Curve, pH: 1 1.90, 2 2.08, 3 2.35, 4 2.65,
 5 2.91, 6 3.22, 7 3.67, 8 4.14, 9 4.70, 10 5.07,
 11 5.58, 12 5.79, 13 6.10, 14 7.26.



formation of a complex with molar ratio $M : L = 1 : 2$. Rather large scatter of the x_{\max} values around the theoretical value, $x_{L\max} = 0.67$, is chiefly caused by distortion of the $\Delta A = f(x_L)$ curves for values $x_L < 0.5$, probably due to hydrolysis of Fe(III) ions at higher pH values or to the presence of a mixture of complexes with molar ratios of $M : L = 1 : 1$ and $1 : 2$ at lower pH values. These distortions also affected the results of the treatment of the continuous variation plots by the JOBCON program⁴⁹.

Reaction of Fe(III) with PAR in Aqueous Medium

In the spectra of solutions with excess Fe(III) ions ($c_M/c_L = 10$, $c_M = 2.016 \cdot 10^{-4} M$, $c_L = 2.016 \cdot 10^{-5} M$ PAR), the ligand absorption bands (LH_3^+ , LH_2 with $\lambda_{\max} = 395$ and 414 nm) disappear and at pH 1–5.5 two new broad absorption maxima of a complex appear at 435 and 532 nm. The curves pass through a sharp isosbestic point at 481 nm and a diffuse point at 440 nm. With increasing pH (> 2.5) a typical double peak appears in the spectrum, with absorption maxima at 495 and 535 nm, and a low-intensity band at 705 nm. In this pH interval the curves pass through a sharp isosbestic point at 441–445 nm.

Equimolar solutions and solutions with small excesses of PAR ($c_M = 2.016 \cdot 10^{-5} M$, $c_L = 2.016 \cdot 10^{-5} M$ or $5.04 \cdot 10^{-5} M$ and $c_M = 1.25 \cdot 10^{-5} M$ and $c_L = 2.50 \cdot 10^{-5} M$) exhibit quite similar spectra. At pH 1–2.65, the absorption maxima of the first complex are located at 437 and 535 nm (IP lie at 488 and 332 nm); at pH 2.7–5.0, the maxima of the second complex are at 495, 535 and 702 nm (IP at 464–470 and 350 nm). Finally at pH > 5 the curves pass through isosbestic points at 340 and 392 nm and exhibit a characteristic double peak at 495 and 535 nm and a low-intensity band at 705 nm. A precipitate separates in the solution at pH > 8 .

The spectra of solutions with large PAR excesses ($c_L = 2.5 \cdot 10^{-5} M$, $c_M = 5.04 \cdot 10^{-6}$ or $2.52 \cdot 10^{-6} M$) contain all the above absorption bands in a pH interval of 1–10, with virtually unchanged position of the absorption maxima (Table V, Fig. 6). The spectra of PAR solutions containing Fe(III), measured at constant pH values of 1.60, 2.0 and 9.50 and at variable concentration ratios of the components, c_M/c_L , have an analogous character. At pH 9.50, the curves for a PAR excess of $c_L/c_M \geq 2$ pass through an IP at 445 and 552 nm and exhibit maxima at 496 and 532 nm, whereas the curves for lower ratios, $c_L/c_M < 1$, do not pass through this point. A precipitate is formed at higher Fe(III) excesses. The maximum at 700 nm is virtually absent in the curves for excess PAR.

The absorbance-pH curves ($c_M/c_L = 10, 5, 1, 1/5$ and $1/10$ for $\lambda = 495, 510, 520, 535$ and 550 nm at $c_L = 2.016 \cdot 10^{-5} M$ and $c_M = 5.04 \cdot 10^{-6}$ or $2.52 \cdot 10^{-6} M$) contain two sufficiently separated formation branches in pH intervals of 1–3 and 3.5–7.5. A red complex of Fe(III) with PAR begins to form at pH ~ 1.1 . The first formation branches of the absorbance-pH curves shift to more acidic regions with increasing

Fe(III) concentration and their well-developed horizontal branches at pH ~ 3 indicate quantitative formation of the first complex, from which protons are dissociated on a further increase in the pH. These other formation branches on the curves for excess Fe(III) are considerably distorted by simultaneous hydrolysis of Fe(III) ions (Fig. 7, 8). The measurement at substantially lower concentrations $c_L = 4 \cdot 10^{-6} \text{ M}$ and $c_M = 2.016 \cdot 10^{-5}$ or $4.032 \cdot 10^{-5} \text{ M}$ also do not yield sufficiently reproducible experimental data.

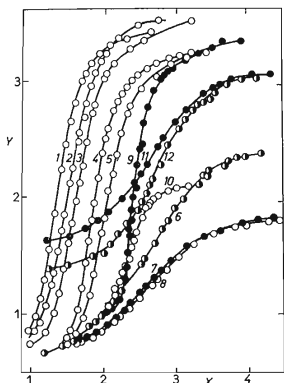


FIG. 7

Absorbance-pH Curves for PAR Solutions with Excess Fe(III) Ions or Excess Ligand $c_L = 2.02 \cdot 10^{-5} \text{ M}$ for curve 1-3, $c_L = 4.00 \cdot 10^{-5}$ for curves 4 and 5, $c_L = 2.00 \cdot 10^{-5} \text{ M}$ for curves 6-8, $c_L = 1.00 \cdot 10^{-4}$ for curves 9, 10 and 12 and $c_L = 5.00 \cdot 10^{-5} \text{ M}$ for curve 11. Curve, $10^4 \cdot c_M$, module x-axis, y-axis: 1 2.02 aa, 2 1.01 aa, 3 0.202 aa, 4 0.403 bb, 5 0.202 bb, 6 0.20 cc, 7 1.00 cc, 8 2.00 cc, 9 0.20 bd, 10 0.10 bd, 11 0.10 dc, 12 0.10 dc; for values 1, 2 and 3 on the x-axis it holds that a: 1, 2, 3, b: 0.50, 1.5, 2.5, c: 2.25, 3.75, 5.00 and d: 0.75, 1.00, 2.25 and for the y-coordinate a: 0.10, 0.15, 0.20, b: 0.10, 0.30, 0.50, c: 0.30, 0.50, 0.70, d: 0.20, 0.40, 0.60.

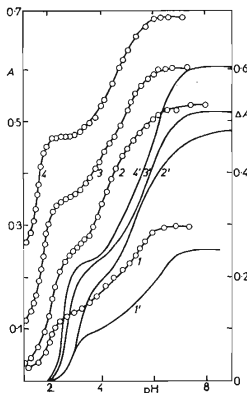


FIG. 8

Absorbance-pH Curves of Fe(III) with PAR with Excess Ligand $A = f(\text{pH})$ and $\Delta A = f(\text{pH})$
 $c_M = 1.008 \cdot 10^{-5} \text{ M}$, 520 nm, t 22.0°C, Curve, $10^5 \cdot c_L \cdot c_L/c_M$: 1 1.00 1, 2 2.00 2, 3 5.00 5, 4 10.1 10; the dashed curves are difference curves $\Delta A = f(\text{pH})$.

TABLE V

Survey of the Optical Characteristics of the Fe(III) Complexes with PAR in Aqueous Solution
 $t = 25^\circ\text{C}$, $I = 0.10\text{M}$ - KNO_3 .

| Conditions | pH | λ_{max} , nm | λ_{ip} , nm |
|-----------------------------|---------------|-----------------------------|----------------------------|
| $c_M/c_L = 10$ | 1-2 | 437, 532 | 435, 484 |
| $c_M = 2.016 \cdot 10^{-5}$ | 3-5 | 493, 532, 702 | 444 |
| $c_M/c_L = 1$ | 1-3 | 434, 523 | 483 |
| $c_M = 2.016 \cdot 10^{-5}$ | 3-9 | 495, 537 | 444 |
| $c_L/c_M = 2$ | 1-3 | 420, 521 | 486 |
| $c_M = 1.25 \cdot 10^{-5}$ | 3-8 | 417, 488, 520, 700 | 391, 455 |
| $c_L/c_M = 5$ | >3 | 413, 485, 520 | 377 |
| $c_M = 2.016 \cdot 10^{-5}$ | ≈ 5.6 | 415, 486, 526 | |
| $c_L/c_M = 10$ | >2.5 | 405, 490, 532 | 270, 445 |
| | >7.5 | 500, 520 | |
| pH 9.50 ^a | | 412, 488, 526 | 352, 445 |
| 1.60 ^b | | 434, 537 | 483, 441, 430 |

^a $c_L = 2.5 \cdot 10^{-5}$ M, $c_M = 0.0 - 1.0 \cdot 10^{-4}$ M, ^b $c_M = 2.016 \cdot 10^{-5}$ M, $c_L = 5 \cdot 10^{-6} - 2 \cdot 10^{-4}$ M

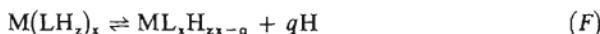
TABLE VI

Average Values of the Equilibrium Constants for the Formation of Complexes of Fe(III) with PAR in Aqueous Solution

| Complex | Equilibrium | $\log^* \beta_{mnx}$ | $(M_m L_n H_x)$ | Conditions |
|--------------------|------------------------------|--|--|--|
| MLH ^c | $[MLH][H]/[M][LH_2]$ | 0.82 ^a 0.65 ^a | 0.80 ^b 0.68 ^b | $A = f(\text{pH})$, $c_M > c_L$ ^c $A = f(c_M)$, pH = 1.60 ^d |
| ML | $[ML][H]/[MLH]$ | 4.37 ^a | 4.38 ^b | $A = f(\text{pH})$, $c_M > c_L$ ^c |
| M(LH) ₂ | $[M(LH)_2][H]^2/[M][LH_2]^2$ | | | $A = f(\text{pH})$, $c_L > c_M$ ^e |

^a Results of the graphical interpretation, ^b results of interpretation by the PRCEK III program;
^c average of values for $c_M/c_L = 10, 5, 1, 10$ and 5 and wavelengths $495, 510, 520, 535$ and 550 nm from the absorbance-pH curves for $c_L = 2.02 \cdot 10^{-5}$ M and $c_L = 4.00 \cdot 10^{-6}$ M; ^d results from the $A = f(c_M)$ curve for pH 1.60; ^e average of values for the $A = f(\text{pH})$ curves with $c_L/c_M = 5$ and 10 and $c_L = 1.00 \cdot 10^{-4}$ M or $c_M = 1.00 \cdot 10^{-5}$ M and wavelengths of $510, 520, 535, 550$ and 570 nm.

The two formation branches of the absorbance-pH curves were treated independently, considering the complex formation directly from the components according to equilibria (A)–(B) in the first part of the curves and conversion of the protonated complexes $M(LH)_x$ for $x = 1$ and 2 to non-protonated ML or ML_2 complexes or to complexes with a lower number of protons ML_2H according to the general equilibrium



and conversion of the MLH complex to the ML_2H complex according to equilibrium



In solutions with excess Fe(III) ions, the protonated MLH complex is formed according to equation (A) with simultaneous dissociation of one proton in the first formation part of the curve ($c_L = 2.016 \cdot 10^{-5} M$, $c_M = 1.008 \cdot 10^{-4}$ and $2.016 \cdot 10^{-4} M$ and for $c_L = 5.04 \cdot 10^{-5} M$, $c_M = 2.52 \cdot 10^{-4} M$ and $5.04 \cdot 10^{-4} M$). The presence of the M_2LH complex was unambiguously excluded using the method of corresponding solutions⁴⁰. In the second part of the absorbance-pH curves, the protonated MLH complex is converted into the ML complex with dissociation of one proton and the dissociation constant values for this reaction are somewhat different because of the above facts (Table VI).

The absorbance-pH curves for ligand excess ($c_M = 1.008 \cdot 10^{-5}$ or $2.016 \cdot 10^{-5} M$ and $c_L = 1.0 \cdot 10^{-4} M$) interpreted by both methods verify the formation of the ML_2H_2 complex at $pH > 1.4$ (the slope of the graphical logarithmic analysis is 1.6 or 2.0) according to equilibrium (B) with dissociation of two protons. The distortion of the c_M/A or $\log(A_{02} - A)/(A - A_{01}) = f(pH)$ dependences at the ends ($pH < 1.4$ and $pH > 2.0$) is probably caused by overlapping of the equilibria of the complex

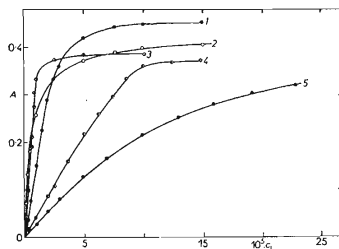
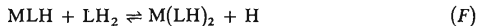


FIG. 9

Absorbance vs Ligand Concentration Curves for Fe(III) Solution with PAR

Curve, λ , pH, $10^5 \cdot c_M$: 1 550 2.00, 2 550 1.60 2.00, 3 535 4.50, 1.00, 4 535 4.00 1.00, 5 550 1.25 2.00.

MLH formation and of its conversion into the ML_2H_2 complex according to reaction mechanisms (A) and (F)



or by formation of the ML_2H_3 complex according to reaction mechanism



in the first part of the absorbance-pH curves and a partial dissociation of the protonated $\text{M}(\text{LH})_2$ complex to the less protonated ML_2H complex in the second part of the curve (pH 2.0-4.2). Both methods of treatment of the further branch of the

TABLE VII

Survey of the Average Values of the Molar Absorption Coefficients for the FeLH , FeL , $\text{Fe}(\text{LH})_2$ and FeL_2 Complexes in the Fe(III)-PAR System

| Complex | 535 | 550 | 510 | 520 | 495 | 570 | Method ^e |
|---|--------|--------|--------|--------|--------|--------|---------------------|
| MLH ^a | 11 795 | 10 085 | 12 290 | 11 880 | 12 830 | — | A |
| | 11 930 | 10 250 | 12 180 | 11 930 | 12 880 | — | B |
| ML ^a | 27 880 | 25 560 | 32 050 | 30 500 | 33 870 | — | A |
| | 27 910 | 26 250 | 31 355 | 30 000 | 33 280 | — | B |
| $\text{M}(\text{LH})_2$ ^b | 21 720 | 18 170 | 17 400 | 18 710 | — | 16 200 | A |
| | 21 545 | 18 375 | 17 610 | 18 880 | — | 16 450 | B |
| ML ₂ ^c | 61 420 | 53 250 | 64 700 | 60 850 | 68 590 | — | A |
| | 61 745 | 55 220 | 63 710 | 61 240 | 67 920 | — | B |
| ML ₂ , ML ₂ H _x ^d | 52 000 | 37 500 | 46 000 | 46 200 | — | 15 000 | B, C |
| ML ₂ H _x | 38 500 | 31 000 | 37 500 | 36 100 | — | 12 000 | B |

^a Average of five values for $c_{\text{M}}/c_{\text{L}} = 10, 5, 1, 10$ and 5 from the absorbance-pH curves for $c_{\text{L}} = 2.02 \cdot 10^{-5}$ or $4.00 \cdot 10^{-6}$ M PAR and $A = f(c_{\text{M}})$ curves for pH 1.60; ^b average value for absorbance-pH curves with $c_{\text{L}}/c_{\text{M}} = 5$ and 10 and $c_{\text{L}} = 1.00 \cdot 10^{-4}$ or $c_{\text{M}} = 1.00 \cdot 10^{-5}$ M and $A = f(c_{\text{L}})$ curves at pH = 1.60, 1.76 and 2.10; ^c average from the absorbance-pH curves $A = f(\text{pH})$ with excess ligand $c_{\text{L}}/c_{\text{M}} = 5, 10, 2, 5$ and 10 for $c_{\text{L}} = 1.00 \cdot 10^{-4}$ M or $c_{\text{M}} = 1.00 \cdot 10^{-5}$ M; ^d results for the $A = f(\text{pH})$ curves for equimolar solutions and $A = f(c_{\text{L}})$ curves for pH 5.00 and continuous variation curves $\Delta A = f(x_{\text{L}})$ for pH 6.0 and 9.0; ^e results for the $A = f(c_{\text{L}})$ curves for pH 4.50. Method A average of the results of the graphical interpretation; method B average of the results of graphical and graphical logarithmic analysis by the PRCEK III program; method C results of treatment by the JOBCON program.

$A = f(\text{pH})$ curves confirm complete deprotonation of the $\text{M}(\text{LH})_2$ complex with formation of the ML_2 complex and dissociation of two protons according to equilibrium



The completely deprotonated ML_2 complex is formed virtually quantitatively at a pH of about 8.5.

The curves of the dependence of the absorbance on the metal concentration, $A = f(c_{\text{M}})$, were only measured for the strongly acidic region at pH 1.60 and $c_{\text{L}} = 5.00 \cdot 10^{-5} \text{M}$. The results of the graphical interpretation confirm the formation of the MLH complex. At higher pH values a precipitate is formed during the measurement of the $A = f(c_{\text{M}})$ curves and the reproducibility is poor. The curves of the absorbance dependence on the ligand concentration $A = f(c_{\text{L}})$ were measured at pH 1.60, 1.76, 1.90, 2.10, 4.50, 5.00 and 5.50 and $c_{\text{M}} = 2.016 \cdot 10^{-5} \text{M}$ or $1.008 \cdot 10^{-5} \text{M}$ Fe(III) (Fig. 9). The formation of complexes with $\text{M} : \text{L} = 1 : 2$ was confirmed in both cases; at pH 1.6–1.9, the molar absorption coefficients and equilibrium constants verify the existence of the $\text{M}(\text{LH})_2$ complex, whereas at pH ≥ 4.5 the results confirm the existence of the ML_2 complex (Tables VI and VII).

The continuous variation plots at pH = 1.50, 2.00, 6.00 and 9.00 and total concentration $c_0 = c_{\text{M}} + c_{\text{L}} = 1.0 \cdot 10^{-4}$ or $5.0 \cdot 10^{-5} \text{M}$ have absorbance maxima at

TABLE VIII

Survey of Basic Characteristics of the Analytical Curves for Fe(III) Systems with TAR and PAR

| Conditions | λ, nm | $\varepsilon \pm 3\sigma$ | $A_{\text{L}} \pm 3\sigma$ | s_{xy}^a |
|--|----------------------|---------------------------|----------------------------|------------|
| PAR | | | | |
| pH 8.5, 0.10M-NH ₄ Cl | 495 | 60 612 \pm 96 | 0.157 \pm 0.002 | 15.3 |
| NH ₄ OH, 4. $\cdot 10^{-4}$ M-PAR | 510 | 58 206 \pm 87 | 0.075 \pm 0.003 | 14.2 |
| $c_{\text{M}} \leq 1 \cdot 10^{-5} \text{M}$ | 535 | 57 250 \pm 64 | 0.018 \pm 0.001 | 13.4 |
| TAR | | | | |
| pH 7.5, 0.10M-NH ₄ Cl | 495 | 32 617 \pm 85 | 0.125 \pm 0.004 | 16.7 |
| NH ₄ OH, 4. $\cdot 10^{-4}$ M-TAR | 530 | 30 176 \pm 77 | 0.101 \pm 0.003 | 15.3 |
| $c_{\text{M}} \leq 2 \cdot 10^{-5} \text{M}$ | 550 | 28 619 \pm 59 | 0.078 \pm 0.002 | 14.0 |

^a Standard deviation for the scattering of points around the regression straight line after recalculation to $s_{xy}(\text{ppm}) = 10^6 \cdot s_{xy} \cdot \text{at. wt./e}$, $s_{xy(A)} = U/(n_p - 2)$, ε molar absorption coefficient value, A_{L} blank values calculated as the intercept on the absorbance axis.

mole fraction $X_L = 0.67$, which confirms the formation of complexes with molar ratios of $M : L = 1 : 2$ over the whole pH interval studied. The curves were treated by the JOBCON program⁴⁹ and the molar absorption coefficients are given in Tables VI and VII for the sake of completeness.

Comparison of the Methods for Determination of Fe(III) with TAR and PAR

The basis of the spectrophotometric methods for the determination of Fe(III) in pure solutions are complexes with molar ratios of $M : L = 1 : 2$, which have higher molar absorption coefficients ($3.3 \cdot 10^4$ for TAR and $6.1 \cdot 10^4$ for PAR). The regions of quantitative formation are very similar for the two complexes (pH > 6 for TAR and pH > 6.5 for PAR), but the LH_2/LH acid-base equilibrium plays a role with TAR ($pK = 6.51$) in this pH region, which renders this reagent much less suitable compared with PAR (the necessity of accurate pH control, high blank absorbance).

The conditions for the determination of Fe(III) were selected as follows: $c_L = 4 \cdot 10^{-4} M$ ligand, pH 7.0–9.5 for PAR and 7.0–8.5 for TAR. Among the buffers tested, tetraborate (max 0.2M), TRIS (max 0.1M) and ammonia (max 0.5M), the latter is most suitable. The analytical curves, $A = f(c_M)$, were treated by the linear least squares method using the STAT program⁵⁰, under the optimum conditions for the determination (pH 8.50 for PAR and 8.50 for TAR, $c_L = 4.0 \cdot 10^{-4} M$, 0.1M- $NH_4Cl + NH_4OH$ and wavelengths of 495, 510 and 535 for PAR and 495, 530 and 550 for TAR, $c_M = 0.10 - 1.20 \cdot 10^{-5} M$ Fe(III)) and the results are given in Table VIII. The use of PAR at 535 nm seems to be optimal; the molar absorption coefficient is not the maximum here, but the blank value and s_{xy} are lower than those at the other wavelengths.

Common acid anions (Cl^- , NO_3^- , ClO_4^- , SO_4^{2-}) do not interfere up to a concentration of 2M, except for SO_4^{2-} , where the absorbance deviation was 2% rel. for $c = 0.2 M$. Analogously, K^+ and Na^+ do not interfere up to a concentration of 2M and NH_4^+ up to a concentration of 0.5M.

REFERENCES

1. Langová-Hniličková M., Sommer L.: *Folia Fac. Sci. Nat. Univ. Brunensis* 9, *Chemia* 6, Opus 2 (1968).
2. Cheng K. L., Bray R. H.: *Anal. Chem.* 27, 782 (1955).
3. Cheng K. L., Goydish B. L.: *Microchem. J.* 7, 166 (1963).
4. Betteridge D.: *Talanta* 13, 1497 (1966).
5. Kozo M., Sekino J.: *Japan Analyst* 13, 213 (1964).
6. Spitzer A., Schweiger A., Popovici V.: *Pharm. Zentralhalle* 104, 83 (1965).
7. Busev A. I., Ivanov V. M., Talipova L. L.: *Zh. Anal. Khim.* 17, 380 (1962).
8. Galik A., Vincourová A.: *Anal. Chim. Acta* 46, 112 (1969).
9. Püschel R.: *Fresenius' Z. Anal. Chem.* 221, 132 (1966).
10. Püschel R., Lassner E., Katzengruber K.: *Fresenius' Z. Anal. Chem.* 223, 414 (1966).

11. Püschel R., Lassner E., Katzengruber K.: *Analyst (London)* **56**, 63 (1967).
12. Shibata S.: *Anal. Chim. Acta* **23**, 367 (1960); **23**, 434 (1960); **25**, 348 (1961).
13. Shibata S., Goto K., Nakashima M.: *Anal. Chim. Acta* **46**, 146 (1969).
14. Iwamoto T.: *Bull. Chem. Soc. Jap.* **34**, 605 (1961).
15. Shijo Y., Takeuchi T.: *Japan Analyst* **13**, 536 (1964); **14**, 511 (1965), *Anal. Abstr.* **1967**, 4693.
16. Cugio I., Ishio S., Shio S.: *Japan Analyst* **14**, 930 (1965).
17. Tanaka M., Funahashi S., Shirai K.: *Anal. Chim. Acta* **39**, 437 (1967).
18. Yotsuyanagi T., Yamashita R., Aomura K.: *Anal. Chem.* **44**, 1091 (1969).
19. Yotsuyanagi T., Yamashita R., Aomura K.: *Japan Analyst* **20**, 1282 (1971); **19**, 981 (1972).
20. Yotsuyanagi T., Goto K., Nagayama M.: *Japan Analyst* **18**, 184 (1969).
21. Nonova D., Evtimova B.: *C. R. Acad. Bulg. Sci.* **26**, 791 (1973).
22. Nonova D., Evtimova B.: *J. Inorg. Nucl. Chem.* **35**, 3581 (1973).
23. Nickles G., Pollard F. H., Samuelson T. J.: *Anal. Chim. Acta* **39**, 37 (1967).
24. Anderson R. G., Nickles G.: *Anal. Chim. Acta* **39**, 469 (1967).
25. Hniličková M., Sommer L.: *This Journal* **26**, 2189 (1961).
26. Hniličková M., Sommer L.: *Talanta* **13**, 667 (1966).
27. Kasiura K.: *Chem. Anal. (Warsaw)* **12**, 401 (1967).
28. Minczewski J., Grzegrzolska E., Kasiura K.: *Chem. Anal. (Warsaw)* **13**, 601 (1968).
29. Matano N., Kawase A.: *Japan Analyst* **9**, 344 (1960).
30. Matano N., Kawase A.: *Trans. Nat. Res. Inst. Metals* **4**, 30 (1962), **4**, 151 (1962), *Chem. Abstr.* **54**, 16 288 g, **55**, 1 021 a.
31. Kawase A.: *Japan Analyst* **13**, 553 (1964).
32. Kawase A.: *Talanta* **12**, 195 (1967).
33. Yanagihara T., Matano N., Kawase A.: *Trans. Nat. Res. Inst. Metals* **1**, 65 (1955).
34. Tanaka H., Yamauchi T.: *Chem. Pharm. Bull.* **12**, 1268 (1964).
35. Jonassen H. B., Chamblin V. C., Wagner V. L. jr., Henry R. A.: *Anal. Chem.* **30**, 1660 (1958).
36. Fulgard M., Jones B.: *Analyst (London)* **84**, 716 (1959).
37. Bowles P. S., Nicks P. S.: *Analyst (London)* **86**, 483 (1961).
38. Langová M., Klabeňová I., Kasiura K., Sommer L.: *This Journal* **41**, 2386 (1976).
39. Věžník M.: *Thesis. J. E. Purkyně University, Brno* 1974.
40. Kubáň V., Sommer L., Havel J.: *This Journal* **40**, 604 (1975).
41. Kubáň V., Sommer L.: *This Journal* **40**, 2032 (1975).
42. Kubáň V., Sommer L.: *Scripta Fac. Sci. Nat. Univ. Brunensis, Chemia* **1**, 6, 17 (1976).
43. Sommer L., Kubáň V., Havel J.: *Folia Fac. Sci. Nat. Univ. Brunensis* **11**, *Chemia* **7**, 9, Opus I (1970).
44. Likussar W., Boltz D. F.: *Anal. Chem.* **43**, 1265 (1971).
45. Likussar W.: *Anal. Chem.* **45**, 1925 (1973).
46. Suchánek M., Šúcha L., Činátllová H.: Unpublished results.
47. Havel J., Kubáň V.: *Scripta Fac. Sci. Nat. Univ. Brunensis, Chemia* **2**, *1*, 87 (1971).
48. Kubáň V.: *Scripta Fac. Sci. Nat. Univ. Brunensis, Chemia* **2**, *2*, 81 (1972).
49. Kubáň V.: Unpublished results.
50. Sommer L., Langová M., Kubáň V.: *Scripta Fac. Sci. Nat. Univ. Brunensis, Chemia* **1**, *8*, 13 (1978).
51. Corsini A., Mai-Ling Yih, Fernando Q., Freiser H.: *Anal. Chem.* **34**, 1090 (1962).
52. Corsini A., Fernando Q., Freiser H.: *Inorg. Chem.* **2**, 224 (1963).
53. Alimarin I. P., Han-Si: *Zh. Anal. Khim.* **18**, 182 (1963).
54. Fuji Y., Ishiguro Y., Shibata S.: *Nagoya Kogyo Gijutsu Shikensho Hokoku* **15**, 171 (1966); *Chem. Abstr.* **65**, 11 319c.
55. Tschitchibabin A. E., Ryazantsev M.: *Zh. Russk. Fiz. Khim. Obshch.* **17**, 1571 (1915).

56. Betteridge D., Todd P. K., Fernando Q., Freiser H.: *Anal. Chem.* **35**, 729 (1963).
57. Reilley C. N.: *Proc. Internat. Sympos. Mikrochem.* **1960**, 479.
58. Traumann V.: *Ann. N.Y. Acad. Sci.* **249**, 31 (1888).
59. Klečková Z., Langová M., Havel J.: *This Journal*, in press.
60. Mushran S. P., Sommer L.: *This Journal* **34**, 3693 (1969).
61. Vošta J.: *Thesis*. J. E. Purkyně University, Brno 1974.
62. Vošta J., Havel J.: Unpublished results.
63. Kaneniwa N., Yoshizawa F., Homma Y.: *Kanazawa Daigaku Jakugokubu Kenkyu Nempo* **10**, 42 (1960); *Chem. Abstr.* **54**, 4541; **55**, 23 155c.
64. Wada H., Nakagawa G.: *Japan Analyst* **14**, 28 (1965); *Chem. Abstr.* **62**, 12 419c.
65. Voštová J., Sommer L.: *This Journal* **41**, 1137 (1976).

Translated by M. Štulíková.